Functional Co-assembly among Subunits of Cyclic-Nucleotide-Activated, Nonselective Cation Channels, and Across Species from Nematode to Human

J. T. Finn,* D. Krautwurst,#§ J. E. Schroeder,# T.-Y. Chen,* R. R. Reed,*#§ and K.-W. Yau*#¶
*Department of Neuroscience, #Howard Hughes Medical Institute, and Departments of §Molecular Biology and Genetics and ¶Ophthalmology, Johns Hopkins University School of Medicine, Baltimore, Maryland 21205 USA

ABSTRACT Cyclic-nucleotide-activated, nonselective cation channels have a central role in sensory transduction. They are most likely tetramers, composed of two subunits (α and β or 1 and 2), with the former, but not the latter, being able to form homomeric cyclic-nucleotide-activated channels. Identified members of this channel family now include, in vertebrates, the rod and cone channels mediating visual transduction and the channel mediating olfactory transduction, each apparently with distinct α- and β-subunits. Homologous channels have also been identified in *Drosophila melanogaster* and *Caenorhabditis elegans*. By co-expressing any combination of two α-subunits, or α- and β-subunits, of this channel family in HEK 293 cells, we have found that they can all co-assemble functionally with each other, including those from fly and nematode. This finding suggests that the subunit members so far identified form a remarkably homogeneous and conserved group, functionally and evolutionarily, with no subfamilies yet identified. The ability to cross-assemble allows these subunits to potentially generate a diversity of heteromeric channels, each with properties specifically suited to a particular cellular function.

INTRODUCTION

Cyclic-nucleotide-activated channels are a recently recognized family of ion channels, the opening of which is activated by cGMP or cAMP (for reviews, see Kaupp, 1995; Finn et al., 1996; Zagotta and Siegelbaum, 1996). The first member, a nonselective cation channel, was identified as a key component of visual transduction in retinal rod photoreceptors (Fesenko et al., 1985; Yau and Nakatani, 1985). Subsequently, similar ion channels were found in retinal cone photoreceptors (Haynes and Yau, 1985) and olfactory receptor neurons (Nakamura and Gold, 1987). These channels now appear to be composed of two subunits (α and β or 1 and 2). There is evidence that the functional channels are tetramers (Gordon and Zagotta, 1995a; Liu et al., 1996), but the stoichiometry between the two subunits is unknown. The α-subunit can form homomeric channels that are activated by cyclic nucleotides. In contrast, the β-subunit cannot form functional cyclic-nucleotide-activated channels by itself, but confers specific properties to the channel complex when co-assembled with the α-subunit (Chen et al., 1993, 1994; Körschen et al., 1995; Bradley et al., 1994; Liman and Buck, 1994). In addition to the cyclic-nucleotide-activated channels that are nonselective among cations, there are others that are activated by cyclic nucleotides but are selective for potassium ions, and still other channels the opening of which is inhibited by cyclic nucleotides (see Finn et al., 1996 for review). The molecular identities of most of these other channels are unknown (but see Yao et al., 1995). They may not necessarily belong to the same group as the rod, cone, and olfactory channels (see Yao et al., 1995 and Discussion here).

The native rod, cone, and olfactory channels show certain differences in properties. For example, the native olfactory channel has roughly the same half-activation constant ($K_{1/2}$), as well as open probability (P_o), for the fully liganded channel, regardless of whether cGMP or cAMP is the ligand, whereas the native rod and cone channels have a $K_{1/2}$ for cAMP that is 1 to 2 orders of magnitude higher than that for cGMP, and a P_o that is considerably smaller when cAMP rather than cGMP is the ligand (for review, see Finn et al., 1996; Zagotta and Siegelbaum, 1996). On the other hand, compared to the native rod channel, the native cone channel appears to have a higher permeability to Ca^{2+} relative to monovalent cations (Perry and McNaughton, 1991; Picones and Korenbrot, 1995). In addition, the native olfactory channel shows a pronounced inhibition by Ca^{2+}-calmodulin, consisting of a ~20-fold increase in $K_{1/2}$ (Chen and Yau, 1994; Balasubramanian et al., 1996), whereas the native rod channel shows a much weaker effect by this modulatory protein (Hsu and Molday, 1993; Gordon et al., 1995; Haynes and Stotz, 1997), and the native cone channel may or may not show any effect at all (Haynes and Stotz, 1997; Hackos and Korenbrot, 1997; see also Bönigk et al., 1996). These various differences in physiological properties are conferred by one or both of the α- and β-subunits (see,

Received for publication 17 September 1997 and in final form 1 December 1997.

Address reprint requests to Dr. King-Wai Yau, Howard Hughes Medical Institute, 9th Floor, Preclinical Teaching Building, Johns Hopkins University School of Medicine, 725 N. Wolfe Street, Baltimore, MD 21205. Tel.: 410-955-1260; Fax: 410-614-3579; E-mail: kwyau@welchlink.welch.jhu.edu.

J. T. Finn's present address is MRC Laboratory for Molecular Cell Biology, University College London, London WC1E 6BT, United Kingdom.

J. E. Schroeder's present address is Howard Hughes Medical Institute, Jones Bridge Rd., Chevy Chase, MD 20815.

T.-Y. Chen's present address is Department of Physiology, National Yang Ming University, Taipei, Taiwan.

0006-3495/98/03/1333/13 $2.00

for example, Kaupp et al., 1989; Dhallan et al., 1990; Weyand et al., 1994; Frings et al., 1995; Liu et al., 1994; Chen et al., 1994; Körschen et al., 1995; Bradley et al., 1994; Liman and Buck, 1994; Goulding et al., 1994; Gordon and Zagotta, 1995b; Tibbs et al., 1997), which, except for the still-unidentified cone-channel β-subunit, appear to be all molecularly distinct among the three sensory channels.

Recent studies involving northern blotting, polymerase chain reaction, cDNA cloning, in situ hybridization, or immunocytochemistry have indicated that the channel subunits composing the native rod, cone, and olfactory channels are not confined to sensory receptor cells, but are also present in other neurons and nonneuronal cells. For example, the rod-channel α-subunit has been found in retinal ganglion cells, hippocampus, kidney, liver, and skeletal muscle (Ahmad et al., 1994; Karlson et al., 1995; Kingston et al., 1996; Feng et al., 1996), the cone-channel α-subunit in pineal gland, testis, kidney, and heart (Weyand et al., 1994; Biel et al., 1994; Bönigk et al., 1996), and the olfactory-channel α-subunit in hippocampus, olfactory bulb, cortex, cerebellum, aorta, and heart (Biel et al., 1993; Kingston et al., 1996; Ruiz et al., 1996; Bradley et al., 1997), even though their functions in these other locations are still largely unclear. In addition, the rod-channel β-subunit has been found in testis, kidney, heart, and brain (Biel et al., 1996), and the olfactory-channel β-subunit in the vomeronasal organ and the hippocampus (Berghard et al., 1996; Bradley et al., 1997). In view of their widespread and overlapping distributions, the question arises whether these channel subunits in the various locations co-assemble with the same compositions and stoichiometries as in the sensory receptor neurons. With each α- and β-subunit appearing to impart some distinct properties, a large number of combinatorial heteromeric channel complexes can, in principle, be generated with characteristics tailored to particular cellular functions, if the various α- and β-subunits can cross-assemble.

To address this question, we have co-expressed different pairs of cyclic-nucleotide-activated channel subunits in HEK 293 cells and examined the physiological properties of the resulting channels in excised, inside-out membrane patches. In addition, we have investigated the degree of conservation among these channel proteins in evolution by co-expressing the vertebrate channel subunits with several known homologs from invertebrates. A single α-subunit (Baumann et al., 1994) and a presumptive β-subunit (J. L. Davis, D. Krautwurst, K.-W. Yau, and R. R. Reed, manuscript in preparation) have been cloned from *Drosophila melanogaster*. Homologs (tax-4 and tax-2) have also been cloned from *C. elegans* (Komatsu et al., 1996; Coburn and Bargmann, 1996). The *Caenorhabditis elegans* channels have been implicated in olfactory, gustatory, and thermal senses (Komatsu et al., 1996; Coburn and Bargmann, 1996), and the *Drosophila* channels are expressed in the eyes and antennae (Baumann et al., 1994), though still of unknown function. In this study, the *Drosophila* α- and β-subunits, as well as the *C. elegans* tax-4, were used. Interestingly, we have found that all of the α- and β-subunits we examined can cross-assemble.

MATERIALS AND METHODS

Transient expression of CNC subunits

The cDNAs used in the experiments included those encoding the α- and β-subunits of the human rod channel (Dhallan et al., 1992; Chen et al., 1993), the α- and β-subunits of the rat olfactory channel (Dhallan et al., 1990; Bradley et al., 1994; Liman and Buck, 1994), the α-subunit of the human cone channel (Yu et al., 1996), the α- and β-subunits of the *Drosophila* cyclic-nucleotide-gated channel (Baumann et al., 1994; J. L. Davis, D. Krautwurst, K.-W. Yau, and R. R. Reed, manuscript in preparation), and the nematode tax-4 channel (Komatsu et al., 1996). The cDNA encoding a point mutant (H418E) of the rod-channel α-subunit was also used. The cDNA encoding the *Drosophila* channel α-subunit was cloned using polymerase chain reaction based on published sequence information (Baumann et al., 1994). The cDNAs encoding the rat olfactory-channel β-subunit and the nematode tax-4 were gifts from K. G. Zinn (Caltech) and I. Mori (Kyushu University, Japan), respectively. All of the cDNAs, except that for tax-4, were subcloned into the pCIS expression vector (Genentech). The tax-4 cDNA was subcloned into the pcDNAI/Amp expression vector (Komatsu et al., 1996).

Human embryonic kidney (HEK) 293 cells were grown on poly-D-lysine-coated coverslips in 10-ml dishes. For experiments involving the expression of one channel subunit, cells were transiently transfected with expression plasmid (10 μg), carrier DNA (pBluescript, 10 μg), and simian virus 40 tumor antigen expression plasmid (RSV-Tag, 1 μg) by the calcium phosphate precipitation method (see, for example, Dhallan et al., 1990). For experiments involving the co-expression of two subunits, carrier DNA was omitted, and a total of 20 μg of expression plasmid was typically added in the following ratios: hRCNCα/rOCNCα, 2:1; rOCNCα/hRCNCβ, 1:1.5; hRCNCα/rOCNCβ, 2:1; rOCNCα/hCCNCα, 1:1.5; hRCNCα(H418E)/dCNCα, 2:1; rOCNCα/dCNCβ, 1:2 or 1:3; hRCNCα/tax-4, 1.5:1; tax-4/hRCNCβ, 1:1. These ratios were somewhat arbitrarily chosen in order to balance different efficiencies of functional expressions observed for the different subunit proteins. In some transfections, the cDNA encoding the jellyfish green fluorescent protein (GFP, 0.3–2 μg) in the pcDNA3 expression vector (Marshall et al., 1995) was also included to help identify transfected cells.

Electrophysiological recordings

Patch-clamp recordings were made from excised, inside-out membrane patches of transfected HEK cells at 48–72 h after transfection. Patch pipettes were made from borosilicate glass capillaries and had tip lumens of ~1 μm in diameter. For experiments involving single-channel recordings, the exterior of the pipette tip was coated with Sylgard elastomer (Dow Corning). The patch pipette contained "0-Ca^{2+}" solution (in mM: 140 NaCl, 5 KCl, 1 Na-EGTA, 1 Na-EDTA, 10 HEPES-NaOH, pH 7.6). Before a membrane seal was established, the bath contained Ringer's solution (in mM: 140 NaCl, 5 KCl, 2 $CaCl_2$, 1 $MgCl_2$, 10 HEPES-NaOH, pH 7.6). A slight positive pressure was maintained inside the pipette to minimize the entry of Ringer's solution. After a seal was established, the bath was switched to 0-Ca^{2+} solution before the patch was excised. cGMP or cAMP at appropriate concentration was added to the 0-Ca^{2+} bath perfusate. For experiments involving Ca^{2+}-calmodulin, the bath solution contained 250 nM calmodulin and 50 μM buffered free Ca^{2+} (0.92 mM $CaCl_2$ and 2 mM sodium nitrilotriacetate) in place of Na-EGTA and Na-EDTA.

All experiments were performed at room temperature. Unless indicated otherwise, all dose-response relations were obtained at +60 mV. For a given patch, the averaged, steady membrane current at each cyclic nucleotide concentration was measured in 50-ms voltage steps from 0 to +60 mV given at 1 Hz. Leakage current in the absence of cyclic nucleotide was

already subtracted. In all of the figures, outward membrane current has a positive sign, and averaged data are given as mean ± S.D. Unless indicated otherwise, the data were low-pass filtered at 2 kHz (8-pole Bessel) and digitized at 5 kHz. Curve fits were performed using a nonlinear least-squares algorithm.

RESULTS

The following terminology has been adopted: RCNC, rod cyclic-nucleotide-activated channel; OCNC, olfactory cyclic-nucleotide-activated channel; CCNC: cone cyclic-nucleotide-activated channel. Because their functions are still unclear, the *Drosophila* channel proteins are referred to simply as CNC, standing for cyclic-nucleotide-activated channel. The prefixes "h," "r," and "d" refer to clones derived from human, rat, and *Drosophila*, respectively. The suffixes "α" and "β" refer to the two subunits. For the *C. elegans* channel α-subunit, the name tax-4 is retained.

In all experiments, HEK 293 cells were transfected with cDNA encoding one or two cyclic-nucleotide-activated channel subunits. For no reason other than convenience, the partial hRCNCβ clone [referred to as hRCNC2b in Chen et al. (1993)] was used instead of the full-length clone; however, the protein encoded by this cDNA shows all of the hallmark properties of that encoded by the full-length clone (Körschen et al., 1995; M. E. Grunwald et al., 1998). Inside-out membrane patches were excised from transfected cells at 48–72 h after transfection and exposed to bath perfusion containing cGMP or cAMP.

Co-expression of hRCNCα and rOCNCα

We first tested whether hRCNCα and rOCNCα can co-assemble into functional channels in HEK cells. The homomeric channels formed by these two proteins have very different half-activation constants (Dhallan et al., 1990, 1992). Their averaged, dose-response relations with cGMP as ligand are shown in Fig. 1 *A, upper left panel*. The continuous curves fitted to the data are from the Hill equation:

$$I(C) = C^n/[C^n + K_{1/2}^n] \quad (1)$$

where $I(C)$ is the normalized current, C is the cyclic nucleotide concentration, $K_{1/2}$ is the half-activation constant, and n is the Hill coefficient. For hRCNCα, $K_{1/2} = 63.2$ μM cGMP, $n = 2.02$ (5 patches), and for rOCNCα, $K_{1/2} = 3.2$ μM cGMP, $n = 1.93$ (4 patches). This wide separation between the two dose-response relations provides a simple test for heteromeric channel formation by the two subunits.

With cells transfected with cDNAs encoding hRCNCα and rOCNCα, dose-response experiments on excised, inside-out patches revealed a range of $K_{1/2}$ values that were intermediate between those for the homomeric channels; at the same time, the n values were significantly lower. In the patch shown in Fig. 1 *A, upper right panel*, for example, $K_{1/2} = 17.5$ μM, $n = 1.57$ (continuous curve). Assuming no heteromeric channel formation, the observed dose-response relation can be predicted from a linear combination of the dose-response relations for the two populations of homomeric channels in the patch:

$$I(C) = fI_{rod}(C) + (1 - f)I_{olf}(C) \quad (2)$$

where $I_{rod}(C)$ and $I_{olf}(C)$ are given by Eq. 1 with respective $K_{1/2}$ and n values for homomeric hRCNCα and rOCNCα channels, and f and $1-f$ are the fractional current contributions from the two channel populations. For illustrative purposes, the calculated relations with f values of 0, 0.2, 0.4, 0.6, 0.8, and 1.0 are shown (*dashed curves*). It is clear that no linear combination can describe the data. In particular, all of the dashed curves show an obvious inflection point that is absent in the experimental relation. Results from two other patches are shown in the lower panels of Fig. 1 *A*, fitted empirically by $K_{1/2} = 15.7$ μM, $n = 1.60$ and $K_{1/2} = 27.5$ μM, $n = 1.68$ (*continuous curves*), respectively. The dashed curves indicate predictions from Eq. 2, with $f = 0.55$ and 0.72, respectively, based on least-squares fits. Again, the predictions from Eq. 2 are poor. Thus, functional heteromeric channels appeared to be formed between hRCNCα and rOCNCα. There might be more than one population of heteromeric channels, depending on whether hRCNCα and rOCNCα can co-assemble with multiple stoichiometries. The heteromeric channels are expected to have $K_{1/2}$ values intermediate between those for the homomeric hRCNCα and rOCNCα channels. At the same time, homomeric channel populations probably were also present on the membrane patch. Thus, several distinct, but closely spaced, dose-response relations may co-exist, and a linear combination of these will lack an obvious inflection point, and also show a small apparent n value, as is the case in Fig. 1 *A*. Furthermore, the proportions of the distinct channel populations are expected to vary from patch to patch, thus explaining the different apparent $K_{1/2}$ values in different experiments.

hRCNCα/rOCNCα co-assembly was also supported by an experiment involving Ca^{2+}-calmodulin. Homomeric rOCNCα, but not homomeric hRCNCα, channels are sensitive to Ca^{2+}-calmodulin, due to binding of Ca^{2+}-calmodulin to a site on the N-terminal of the rOCNCα protein and affecting channel gating (Chen and Yau, 1994; Liu et al., 1994). Fig. 1 *B, left panel*, shows that, in the presence of 50 μM Ca^{2+} and 250 nM calmodulin, the $K_{1/2}$ for cGMP increases by ~10-fold for homomeric rOCNCα. Fig. 1 *B, right panel*, shows that an increase in the $K_{1/2}$ for cGMP due to Ca^{2+}-calmodulin was likewise observed in a hRCNCα/rOCNCα co-expression experiment. Assuming no formation of heteromeric channels, we fitted a scaled version of the dose-response relation for homomeric rOCNCα based on the left panel to the two lowest data points at the foot of the control dose-response relation in the right panel (*curve 1*), from which the presumptive contribution by homomeric hRCNCα (not shown) could be obtained by subtraction. In the presence of Ca^{2+}-calmodulin, we obtained curve 2 by first shifting the rOCNCα contribution according to the

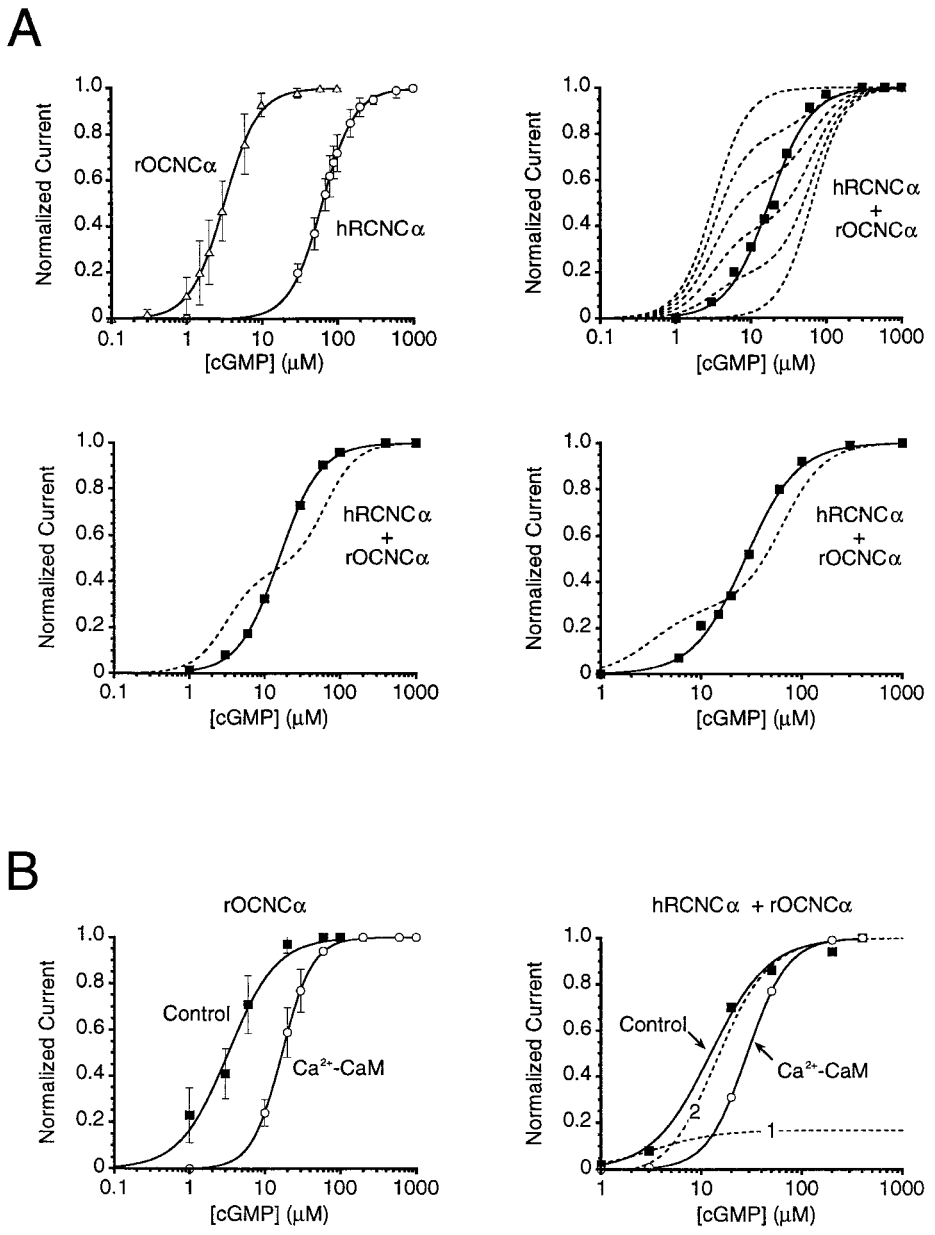

FIGURE 1 Co-assembly of hRCNCα and rOCNCα. (*A*) Upper left, cGMP dose-response relations for homomeric hRCNCα and rOCNCα channels. Averaged data from 5 patches for hRCNCα and from 4 patches for rOCNCα, normalized with respect to the maximum cGMP-induced current in each case. Error bars are standard deviations. Continuous curves are Eq. 1 with $K_{1/2} = 63.2$ μM, $n = 2.02$ for homomeric hRCNCα, and $K_{1/2} = 3.2$ μM, $n = 1.93$ for homomeric rOCNCα. Upper right, cGMP dose-response relation obtained from an inside-out patch excised from a cell co-transfected with hRCNCα and rOCNCα cDNA. Continuous curve is Eq. 1, with $K_{1/2} = 17.5$ μM, $n = 1.57$. Dashed curves are drawn from Eq. 2, with f values of 0, 0.2, 0.4, 0.6, 0.8, and 1.0. Lower panels, results from two other excised patches. Continuous curves are Eq. 1, with $K_{1/2} = 15.7$ μM, $n = 1.60$ (*left*) and $K_{1/2} = 27.5$ μM, $n = 1.68$ (*right*). Dashed curves are best fits from Eq. 2, with $f = 0.55$ (*left*) and 0.72 (*right*). (*B*) Effect of Ca^{2+}-calmodulin. Left, cGMP dose-response relations for homomeric rOCNCα in control conditions and in the presence of 250 nM calmodulin and 50 μM buffered free Ca^{2+}. Averaged data from 3 patches. Continuous curves are Eq. 1 with $K_{1/2} = 3.3$ μM, $n = 1.36$ and $K_{1/2} = 17.0$ μM, $n = 2.16$, respectively. Right, cGMP dose-response relations for co-expressed hRCNCα and rOCNCα in control conditions and in the presence of Ca^{2+}-calmodulin. Data are all from one patch. Continuous curves are Eq. 1, with $K_{1/2} = 12.4$ μM, $n = 1.52$ and $K_{1/2} = 28.8$ μM, $n = 2.20$, respectively. Curve 1, presumptive contribution from homomeric rOCNCα in control conditions (scaled version of control curve in left panel fitted to the lowest two data points of the experimental dose-response relation) if no heteromeric channels were formed. Curve 2, predicted position of overall dose-response relation in the presence of Ca^{2+}-calmodulin (see text for details).

results in the left panel and then summing with the homomeric hRCNCα component. This predicted relation is considerably different from the observed relation (*open circles*), suggesting that hRCNCα and rOCNCα must co-assemble. The much larger-than-predicted shift of the observed relation indicates that Ca^{2+}-calmodulin also modulates heteromeric hRCNCα/rOCNCα channels. In other words, not every subunit forming the channel complex needs to have a

Ca^{2+}-calmodulin-binding site in order for modulation to take place. This finding is consistent with what was previously found for the native rod channel, where Ca^{2+}-calmodulin acts by binding to the β-subunit alone (Chen et al., 1994).

Co-expression of rOCNCα and hRCNCβ

Next, we asked whether rOCNCα and hRCNCβ could co-assemble. Because hRCNCβ by itself cannot form channels that are activated by cGMP (Chen et al., 1993), any dose-response relation obtained in a co-expression experiment that is significantly different from that for the homomeric rOCNCα channel should reflect heteromeric channel formation. Indeed, this is the case. In Fig. 2*A*, *left* and *right panels*, the dose-response relations obtained from two excised patches containing co-expressed rOCNCα and hRCNCβ had $K_{1/2}$ values for cGMP that were considerably higher than the value for the homomeric rOCNCα channel (*dashed curve*). The shift to higher cGMP concentrations was expected from the presence of a RCNC subunit. It is not clear whether rOCNCα and hRCNCβ (or, for that matter, hRCNCα and hRCNCβ in the native rod channel) can co-assemble with more than one stoichiometry.

The native rod channel shows a high sensitivity to the blocker *L-cis*-diltiazem, a property conferred by RCNCβ

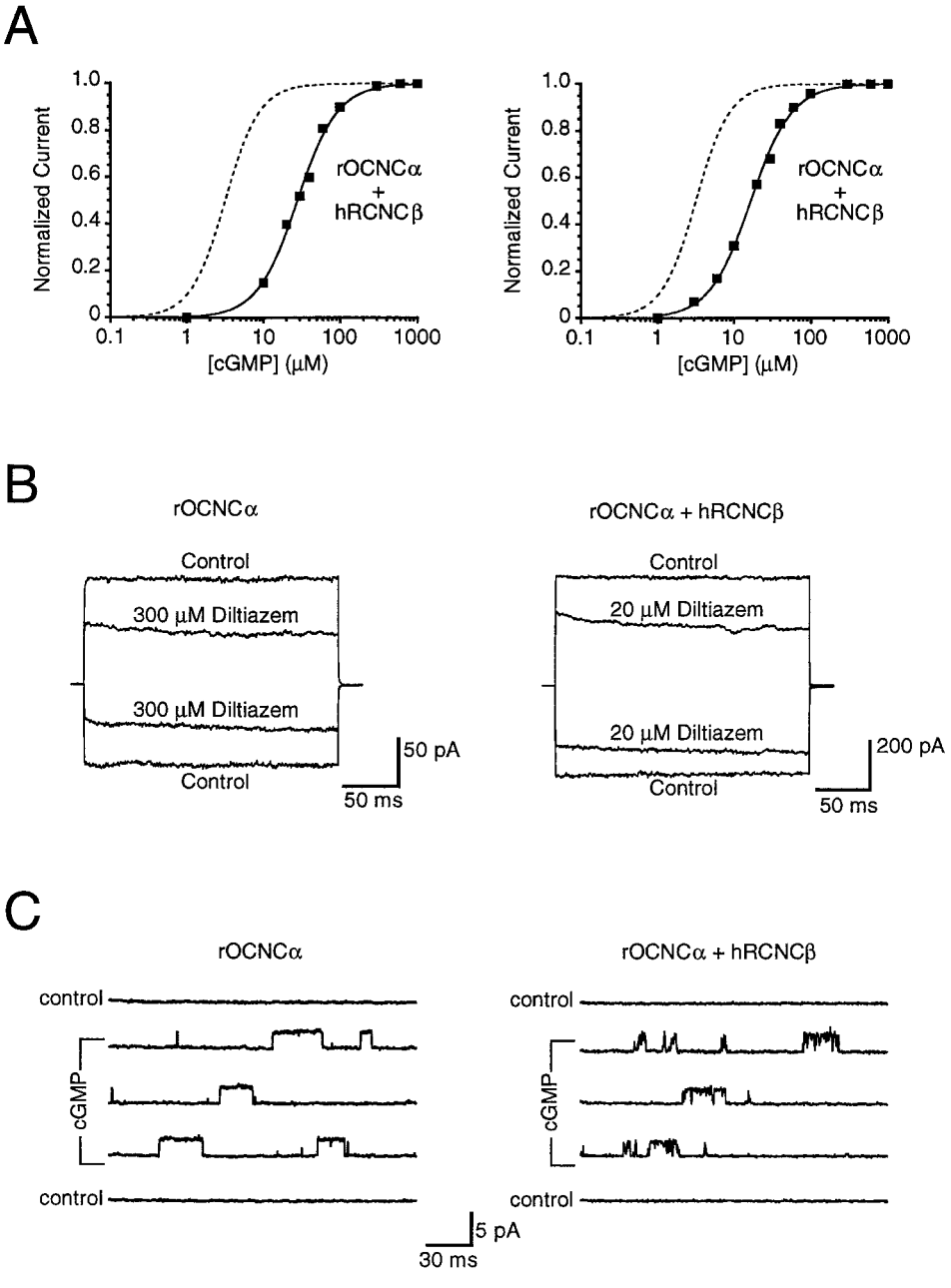

FIGURE 2 Co-assembly of rOCNCα and hRCNCβ. (*A*) Left and right panels show cGMP dose-response relations from two patches, showing an increase in $K_{1/2}$ relative to homomeric rOCNCα. Continuous curves are Eq. 1, with $K_{1/2}$ = 27.8 μM, n = 1.65 (*left*), and $K_{1/2}$ = 16.7 μM, n = 1.60 (*right*). Dashed curves are identical to continuous curves for homomeric rOCNCα in Fig. 1 *A*, top left. (*B*) Increase in sensitivity to *L-cis*-diltiazem with hRCNCβ present. In both panels, each trace represents the average of 5 to 10 voltage steps (given at 1 Hz) from 0 to +60 mV or −60 mV, in the presence of 1 mM cGMP with or without the blocker. Leakage current measured in the absence of cGMP has been subtracted. (*C*) The presence of hRCNCβ produced flickery single-channel openings, +60 mV, given in 300-ms voltage steps from 0 mV. Nominal cGMP concentrations were 0.3 μM (*left*) and 1 μM (*right*). Recordings were low-pass filtered at 2 kHz (8-pole Bessel) and digitized at 10 kHz.

(Chen et al., 1993). hRCNCβ likewise increases the sensitivity of rOCNCα to this blocker (Fig. 2 *B*). At +60 mV, the sensitivity of rOCNCα to diltiazem increased by ~15-fold in the presence of hRCNCβ, with the IC_{50} decreasing from ~300 μM to 20 μM. This change in IC_{50} is smaller than that observed for the effect of hRCNCβ on hRCNCα (IC_{50} decreasing from 100 μM to 1 μM at +60 mV; see Chen et al., 1993), perhaps reflecting a difference between the RCNCα/RCNCβ and OCNCα/RCNCβ complexes in interacting with diltiazem.

Finally, at the single-channel level, the heteromeric rOCNCα/hRCNCβ channels showed flickery transitions between the open and closed states, quite different from the behavior of the homomeric rOCNCα channels (Fig. 2 *C*). The same characteristic was previously observed when hRCNCα and hRCNCβ were co-expressed, comprising the native rod channel (Chen et al., 1993).

Co-expression of hRCNCα and rOCNCβ

We asked the reciprocal question, namely whether hRCNCα could co-assemble with rOCNCβ. The strategy was similar to that described immediately above because OCNCβ, like RCNCβ, cannot form homomeric channels that are activated by cyclic nucleotides (Bradley et al., 1994; Liman and Buck, 1994). In Fig. 3 *A*, the cGMP dose-response relations obtained from two patches in co-transfection experiments clearly deviated from that for homomeric hRCNCα channels (*dashed curve*). Unlike that in Fig.

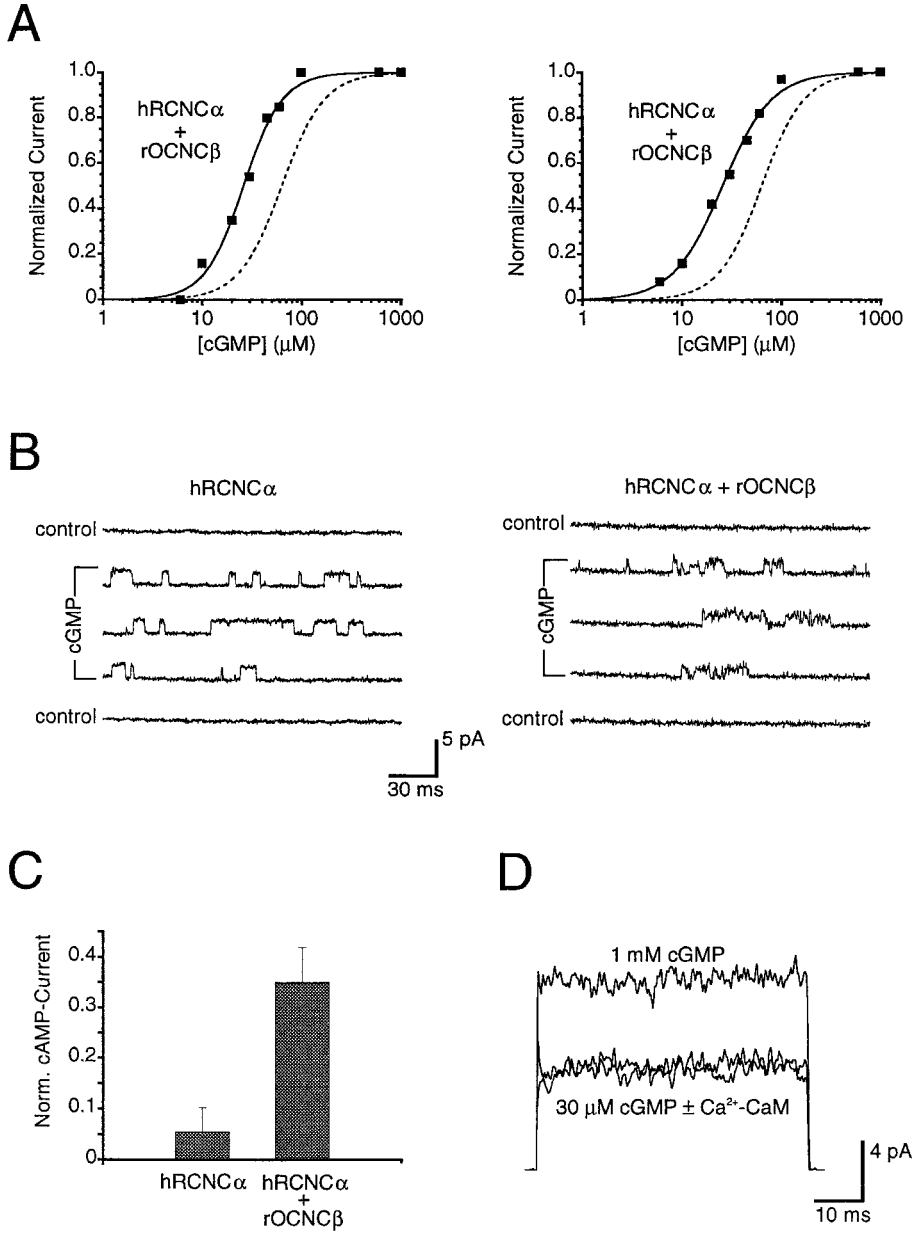

FIGURE 3 Co-assembly of hRCNCα and rOCNCβ. (*A*) Left and right panels show cGMP dose-response relations from two patches, showing a decrease in $K_{1/2}$ relative to homomeric hRCNCα. Continuous curves are Eq. 1, with $K_{1/2}$ = 26.2 μM, n = 2.24 (*left*), and $K_{1/2}$ = 25.5 μM, n = 1.75 (*right*). Dashed curves are identical to continuous curves for homomeric hRCNCα in Fig. 1 *A*, top left. (*B*) The presence of rOCNCβ produced flickery single-channel openings, +60 mV, given in 300-ms voltage steps from 0. Nominal cGMP concentrations were 10 μM (*left*) and 6 μM (*right*). The same signal processing is used as in Fig. 2 *C*. (*C*) The presence of rOCNCβ increased the current induced by 25 mM cAMP relative to that elicited by 1 mM cGMP. Values are 0.055 ± 0.048 for hRCNCα expressed alone (3 patches) and 0.35 ± 0.07 for hRCNCα and rOCNCβ expressed together (3 patches). Because P_o for homomeric hRCNCα is at most 1.0 with cGMP as ligand, its P_o for cAMP must be at most 0.055 (given that the single-channel currents induced by both cyclic nucleotides are similar; see Chen and Yau, 1994). (*D*) Lack of modulation by Ca^{2+}-calmodulin on the heteromeric hRCNCα/rOCNCβ channel. Each trace represents the average of 5 voltage steps (at 1 Hz) from 0 to +60 mV in the presence of 1 mM cGMP or 30 μM cGMP with either 1 mM EGTA/EDTA or 250 nM calmodulin/50 μM buffered free Ca^{2+}. Leakage current measured in the absence of cGMP has been subtracted.

2 *A*, the shift in this case is toward lower cGMP concentrations, again as might be expected from the presence of an OCNC subunit. Flickery openings were likewise observed for the heteromeric channels (Fig. 3 *B*), a feature that rOCNCβ, like RCNCβ, confers (Bradley et al., 1994; Liman and Buck, 1994).

The homomeric rOCNCα channel has a $K_{1/2}$ for cAMP that is ~30-fold higher than that for cGMP (Dhallan et al., 1990). On the other hand, for the heteromeric rOCNCα/rOCNCβ channel, the $K_{1/2}$ for cAMP decreases to a value close to that for cGMP (Bradley et al., 1994; Liman and Buck, 1994). In both situations, however, the maximum currents induced by cGMP and cAMP are very similar (see Fig. 4, *upper left panel*, for homomeric rOCNCα). Thus, it is not clear whether the decrease in $K_{1/2}$ for cAMP with rOCNCβ present is due directly to a higher affinity between cAMP and the binding sites or indirectly to an increase in the P_o of the liganded channel, owing to the coupling between the kinetic steps of ligand binding and channel gating (Liu et al., 1994; Goulding et al., 1994; Gordon and Zagotta, 1995; Tibbs et al., 1997). In particular, because the P_o of the liganded rOCNCα homomer is already close to unity (~0.94, see Liu et al., 1994), any increase in P_o, while affecting the $K_{1/2}$, will have a minimal effect on the maximum cAMP-induced current. The hRCNCα/rOCNCβ heteromer offers an opportunity to examine this question because the P_o of the hRCNCα homomer with cAMP bound is under 0.06 (see Fig. 3 *C* legend). Indeed, on average, the maximum cAMP-induced current/maximum cGMP-induced current ratio was 7-fold higher for hRCNC1α/rOCNCβ co-expression than for hRCNCα expressed alone (Fig. 3 *C*). Thus, undoubtedly, the presence of rOCNCβ decreases the $K_{1/2}$ for cAMP at least in part by affecting gating, i.e., promoting the open state of the liganded channel.

Finally, the native olfactory channel shows a strong modulation by Ca^{2+}-calmodulin (Chen and Yau, 1994; Balasubramanian et al., 1996). Whether OCNCβ in this native channel complex also confers part of the Ca^{2+}-calmodulin effect, however, has not been examined. The hRCNCα/rOCNCβ heteromer again allows this question to be addressed because hRCNCα is not modulated by Ca^{2+}-calmodulin (Chen et al., 1994). In Fig. 3 *D* it is obvious that this heteromeric channel does not show any sensitivity to Ca^{2+}-calmodulin, indicating that OCNCβ, unlike OCNCα (and RCNCβ; see Chen et al., 1994), does not show this modulatory property.

We have not tested whether rOCNCβ can enhance the sensitivity of RCNCα to *L-cis*-diltiazem, as hRCNCβ does (Chen et al., 1993). However, even if present, this effect is likely to be smaller because, as described above, the IC_{50} for homomeric OCNCα channels is ~300 μM at +60 mV (Fig. 2 *B*), which is not greatly different from the ~70 μM at the same voltage found for the native olfactory channel (composed of OCNCα and OCNCβ) in frog (Frings et al., 1992).

Co-expression of rOCNCα and hCCNCα

The homomeric rOCNCα and hCCNCα channels have cGMP dose-response relations relatively close to each other ($K_{1/2}$ values of ~3 μM and 18 μM cGMP, respectively; see Fig. 1 *A* here and Yu et al., 1996), making it difficult to use

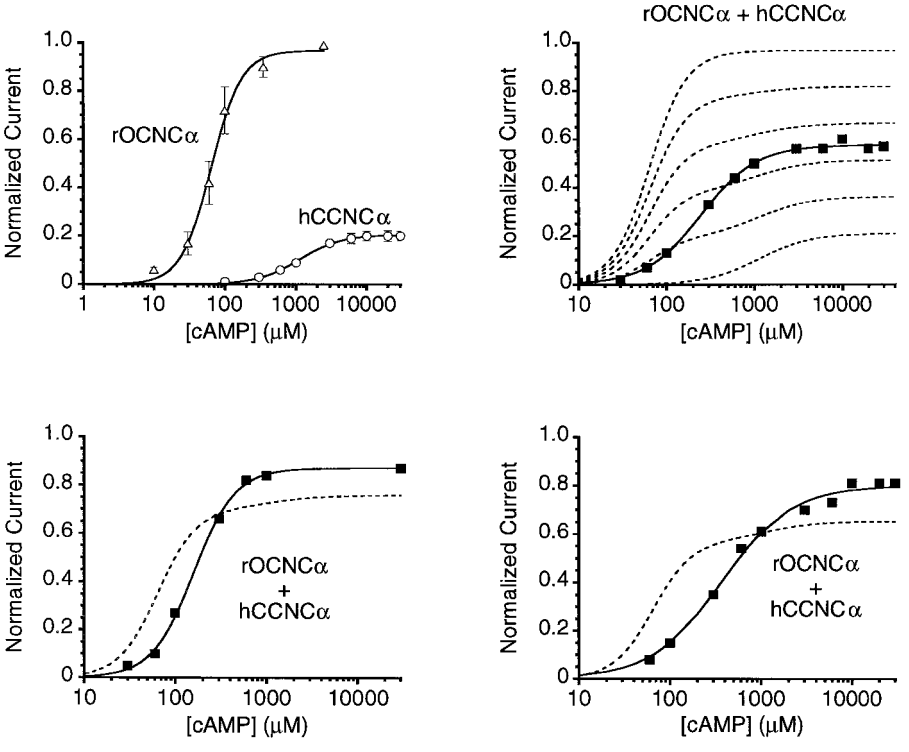

FIGURE 4 Co-assembly of rOCNCα and hCCNCα. Upper left, cAMP dose-response relations for homomeric rOCNCα and hCCNCα channels, normalized against the respective maximum cGMP-induced currents. Averaged data from 5 patches for rOCNCα and from 4 patches for hCCNCα. Continuous curves are Eq. 1, with $K_{1/2}$ = 64.5 μM, n = 2.04, scaling factor = 0.97 for homomeric rOCNCα, and $K_{1/2}$ = 1.11 mM, n = 1.48, scaling factor = 0.21 for homomeric hCCNCα. Upper right, cAMP dose-response relation from one patch in a co-expression experiment, again normalized against the maximum cGMP-induced current. The continuous curve is Eq. 1, with $K_{1/2}$ = 248 μM, n = 1.39, scaling factor = 0.58. Dashed curves are Eq. 3, with values of 0, 0.2, 0.4, 0.6, 0.8, and 1.0. Lower panels, results from two other patches. Continuous curves correspond to Eq. 1, with $K_{1/2}$ = 159 μM, n = 1.89, scaling factor = 0.87 (*left*), and $K_{1/2}$ = 363 μM, n = 1.13, scaling factor = 0.80 (*right*). Dashed curves are best fits from Eq. 3, with f = 0.27 (*left*) and 0.41 (*right*).

the linear-combination method as a test for rOCNCα/hCCNCα co-assembly with cGMP as ligand. However, the corresponding cAMP dose-response relations for the two homomeric channels are very different ($K_{1/2}$ values of ~64 μM and 1.1 mM cAMP, respectively; see Fig. 4, *upper left panel*), so we chose cAMP as the ligand for our experiments. The maximum current inducible by cAMP relative to that by cGMP for homomeric hCCNCα is also greatly different (a ratio of 0.21, see Fig. 4, *upper left panel*), permitting an even more sensitive test using the linear-combination method. As an example, in Fig. 4, *upper right panel*, the cAMP dose-response relation, with amplitude normalized with respect to the maximum cGMP-induced current, is shown for an excised patch from a rOCNCα/hCCNCα co-expression experiment. The dashed curves are calculated according to the equation:

$$I(C) = 0.21 \times f I_{\text{cone}}(C) + 0.97 \times (1 - f) I_{\text{olf}}(C) \quad (3)$$

where $I_{\text{cone}}(C)$ and $I_{\text{olf}}(C)$ are given by normalized Hill equations identical to Eq. 1, f and $1-f$ are the respective fractions of maximum cGMP-induced current contributed by the two populations of homomeric channels, the scaling factors 0.21 and 0.97 reflect the respective maximum cAMP-induced current/maximum cGMP-induced current ratios for the two channels, and C is cAMP concentration. Again, the fit to the experimental data is poor regardless of f value (0, 0.2, 0.4, 0.6, 0.8, and 1.0 shown) indicative of co-assembly between the two subunits. The lower panels of Fig. 4 show two more examples of this type of experiment, along with the best fits based on Eq. 3, leading to a similar conclusion.

The fact that OCNCα and CCNCα can co-assemble, as do OCNCα and RCNCα, suggests that RCNCα and CCNCα can likewise do so, even though we have not tested this possibility.

Co-expressions of hRCNCα and dCNCα, rOCNCα and dCNCβ, hRCNCα and tax-4, tax-4 and hRCNCβ

To examine the degree of evolutionary conservation within the cyclic-nucleotide-activated channel family, we tested for co-assembly between the vertebrate subunit proteins and those from fly and nematode. For the dCNCα/hRCNCα experiments, instead of using the wild-type hRCNCα, we took advantage of a point mutant of hRCNCα (H418E) that we recently found to have an even higher $K_{1/2}$ for cGMP of 146 μM (J. T. Finn, H. Zhong, J. Li, and K.-W. Yau, manuscript in preparation) compared to the low value of 3.4 μM cGMP for dCNCα (Fig. 5 *A*, *left upper panel*). This wide difference makes the linear-combination method even more suitable as a test for co-assembly. In the upper right and the two lower panels of Fig. 5 *A*, measurements from three patches are shown and displayed in the same format as in Fig. 1 *A*. The disparity between the data and the linear-combination curves clearly indicate that the two channel proteins can co-assemble.

Next, we tested for rOCNCα/dCNCβ co-assembly. Because dCNCβ, like other β-subunits described above, do not form homomeric channels that can be activated by cyclic nucleotides (J. L. Davis, D. Krautwurst, K.-W. Yau, and R. R. Reed, manuscript in preparation), co-assembly can be revealed by any significant difference in observed channel properties from the homomeric rOCNCα channel as described above. With cGMP as ligand, the $K_{1/2}$ appeared to be slightly higher for rOCNCα/dCNCβ co-expression than rOCNCα expressed alone (data not shown); however, this small difference detected by comparing across patches was judged to be inconclusive. Instead, we decided to compare, on the same patch, the maximum cGMP- and cAMP-induced currents. As shown in Fig. 5 *B*, *left panel*, whereas high concentrations of cGMP and cAMP produced practically identical currents for homomeric rOCNCα channels (*upper trace*), the maximum cAMP-induced current was ~85% of the maximum cGMP-induced current in an rOCNCα/dCNCβ co-expression experiment (*lower trace*). Averaged dose-response data from multiple experiments with cAMP as ligand also suggested co-assembly (Fig. 5 *B*, *right panel*). The heteromeric rOCNCα/dCNCβ channel may have a maximum cAMP-induced current/maximum cGMP-induced current ratio even lower than the averaged value of 0.76 indicated in the dose-response data because of possible bias from the presence of homomeric rOCNCα channels. Associated with the change in maximum cAMP-induced current there was a slight increase in the $K_{1/2}$ for cAMP, as would be expected from a change in P_o. Instead of rOCNCα, hRCNCα could have been used to test for co-assembly with dCNCβ, but the expression levels of rOCNCα and dCNCβ appeared to be more comparable to each other.

Finally, we tested the ability of tax-4 from nematode to co-assemble with the vertebrate proteins. Because tax-4 has a very low $K_{1/2}$ for cGMP of ~0.4 μM (Komatsu et al., 1996; also Fig. 6 *A*, *upper left panel*, here), we used hRCNCα for assay with the linear-combination method. Co-expression experiments (Fig. 6 *A*, *upper right* and the two *lower panels*) clearly indicated that tax-4 could co-assemble with hRCNCα. In occasional patches there was a noticeable inflection point in the dose-response relation (for example, indicated by the *arrow* in the lower right panel in Fig. 6 *A*), a feature that we almost never detected in co-expression experiments involving other α-subunits. This inflection point may simply result from the fact that homomeric tax-4 channels have such a low $K_{1/2}$ for cGMP that their contribution to the overall dose-response relation, even in mixed channel populations, is still discernible. We have also employed hRCNCβ to check for co-assembly with tax-4 based on the shift in the cGMP dose-response relation and the appearance of flickery openings in co-expression experiments. Both tests indicated co-assembly (Fig. 6 *B*).

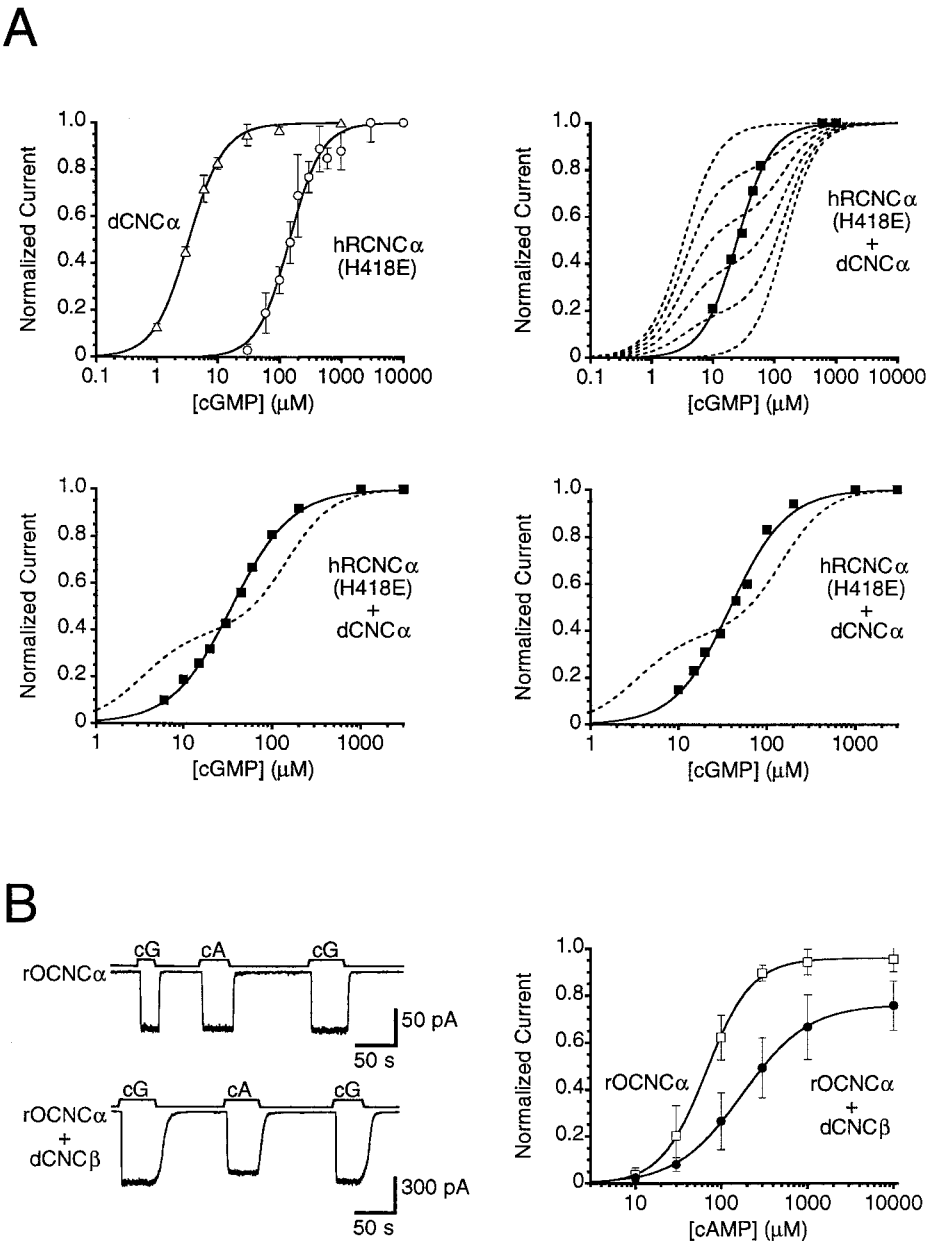

FIGURE 5 hRCNCα/dCNCα and rOCNCα/dCNCβ co-assemblies. (*A*) Co-assembly of hRCNCα and dCNCα. Upper left, normalized cGMP dose-response relations for homomeric dCNCα and hRCNCα(H418E) channels. Averaged data from 3 patches for dCNCα and 4 patches for hRCNCα(H418E). Continuous curves are Eq. 1, with $K_{1/2}$ = 3.39 μM, n = 1.51 for homomeric dCNCα and $K_{1/2}$ = 146 μM, n = 1.67 for homomeric hRCNCα(H418E). Upper right, cGMP dose-response relation from a patch in a co-expression experiment. The continuous curve is Eq. 1, with $K_{1/2}$ = 25.2 μM, n = 1.54. The dashed curves are from a linear-combination expression similar to Eq. 2, with the fraction of total current contributed by hRCNCα(H418E) being 0, 0.2, 0.4, 0.6, 0.8, and 1.0, respectively. Lower panels, results from two other patches. Continuous curves are Eq. 1, with $K_{1/2}$ = 35.1 μM, n = 1.29 (*left*) and $K_{1/2}$ = 38.9 μM, n = 1.38 (*right*). Dashed curves are best fits based on linear combination as above, with the fraction of total current contributed by dCNCα = 0.40 (*left*) and 0.39 (*right*). (*B*) Co-assembly of rOCNCα and dCNCβ. Left, comparison of maximum currents induced by cGMP (10 mM) and cAMP (10 mM) for a patch containing rOCNCα and another patch containing rOCNCα + dCNCβ; −60 mV. Right, averaged cAMP dose-response relations for rOCNCα (8 patches) and rOCNCα + dCNCβ (11 patches), normalized against the respective maximum current induced by cGMP (10 mM); −60 mV. Continuous curves are Eq. 1, with $K_{1/2}$ = 67.6 μM, n = 1.66, scaling factor = 0.96, and $K_{1/2}$ = 177 μM, n = 1.15, scaling factor = 0.76.

DISCUSSION

Apart from elucidating some of their properties, the co-expression experiments have indicated that all tested cyclic-nucleotide-activated, nonselective cation channel subunits—from nematode to human—can co-assemble with each other to form functional channels. This is probably the first demonstration of homologous ion channel subunits from two species as evolutionarily diverged as nematode and human shown to be able to co-assemble functionally. Previously, co-assembly was found between *Shaker* potassium channel subunits from fly and rat (Isacoff et al., 1990). In Table 1 we depict the degrees of amino acid identity among the various subunits tested. Considering that the various α-subunits can all cross-assemble, it is perhaps not too surprising that they are quite homologous to each other, with the percentages of identity ranging from 40% to 62%. On the other hand, it is somewhat surprising that, even though the β-subunits as a group share very limited homology among themselves, they can substitute for each other in assembling with the α-subunits. For example, dCNCβ bears only 29% identity to rOCNCβ, but can co-assemble with the latter's native partner, rOCNCα. Because of the limited homologies among the β-subunits, clues about any functional domains important for assembly may be derivable from sequence comparisons. At present the β-subunit of the cone channel has not been identified at the molecular level. At the same time, we have not examined in this study the tax-2 channel protein, which is presumably the corresponding β-subunit of the *C. elegans* channel (Coburn and Bargmann, 1996). However, based on the findings reported here,

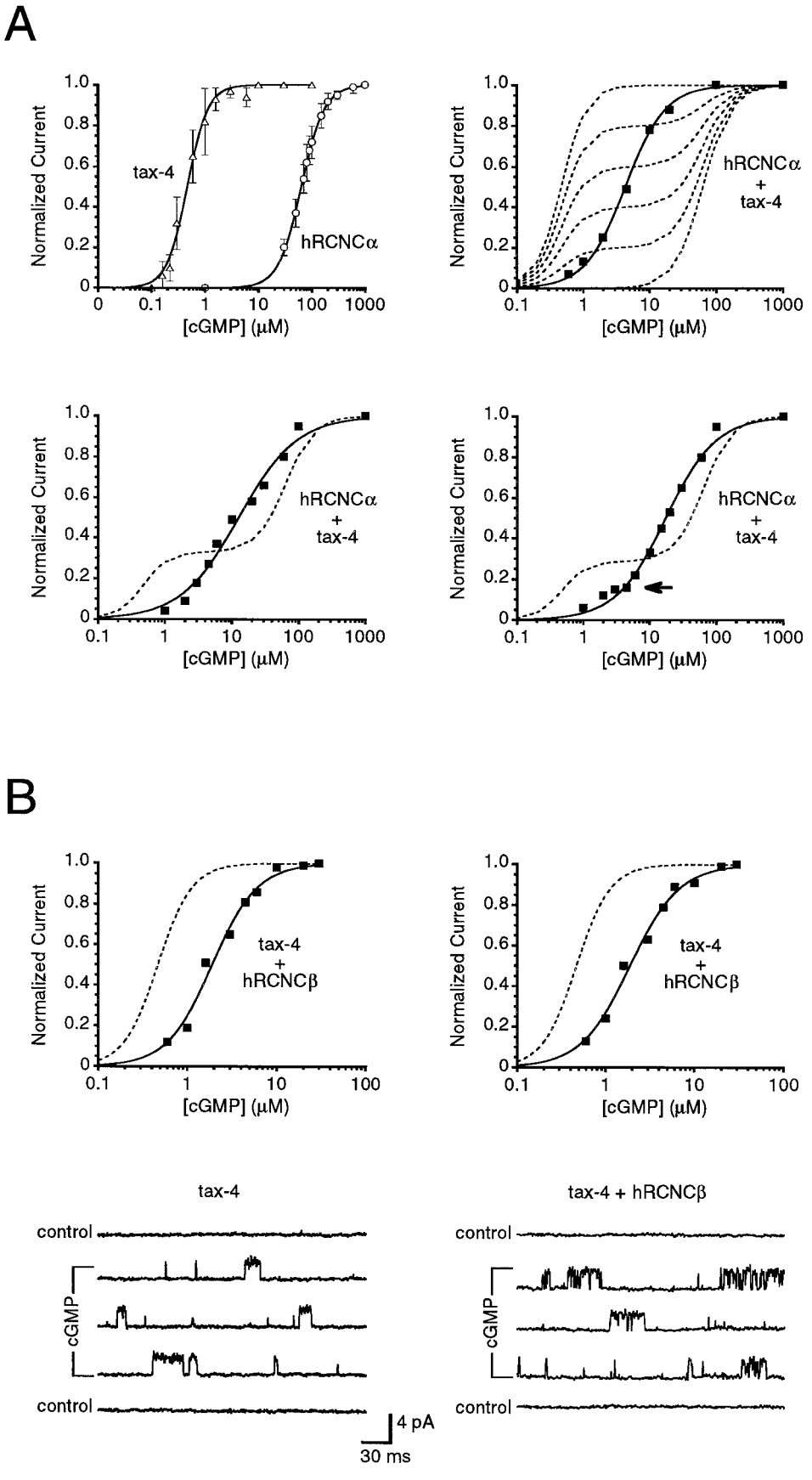

FIGURE 6 hRCNCα/tax-4 and tax-4/hRCNCβ co-assemblies. (*A*) Co-assembly of hRCNCα and tax-4. Upper left, normalized cGMP dose-response relations for homomeric tax-4 and hRCNCα channels. Averaged data from 5 patches for both. Continuous curves are Eq. 1, with $K_{1/2}$ = 0.470 μM, n = 2.27 for homomeric tax-4 and $K_{1/2}$ = 63.2 μM, n = 2.02 for homomeric hRCNCα (see Fig. 1 *A*, *upper left*). Upper right, cGMP dose-response relation from a patch in a co-expression experiment. Continuous curve is Eq. 1, with $K_{1/2}$ = 4.32 μM, n = 1.45. Dashed curves are from a linear-combination expression similar to Eq. 2, with the fraction of total current contributed by hRCNCα being 0, 0.2, 0.4, 0.6, 0.8, and 1.0, respectively. Lower panels, results from two other patches. Continuous curves are Eq. 1, with $K_{1/2}$ = 12.6 μM, n = 1.01 (*left*), and $K_{1/2}$ = 17.3 μM, n = 1.16 (*right*). Dashed curves are best fits based on linear combinations, with the fraction of total current contributed by tax-4 = 0.33 (*left*) and 0.29 (*right*). The arrow in the lower right panel indicates sign of an inflection point in the experimental dose-response relation. (*B*) Co-assembly of tax-4 and hRCNCβ. Upper left and right panels, cGMP dose-response relations from two patches, showing an increase in $K_{1/2}$ relative to homomeric tax-4. Continuous curves are Eq. 1, with $K_{1/2}$ = 1.90 μM, n = 1.73 (*left*), and $K_{1/2}$ = 1.89 μM, n = 1.57 (*right*). Dashed curves are identical to continuous curves for homomeric tax-4 in the upper left panel. Lower panels, the presence of hRCNCβ produced flickery single-channel openings, +60 mV. Nominal cGMP concentrations were 0.06 μM (*left*) and 0.1 μM (*right*). The same protocols and data processing are used as in Fig. 2 *C*.

TABLE 1 Amino acid-identity comparisons among various cyclic-nucleotide-activated, nonselective cation channel subunits

	Percent Identities of CNC Subunits							
Identity	hRCNCα	rOCNCα	hCCNCα	dCNCα	tax-4	hRCNCβ*	rOCNCβ	dCNCβ
dCNCβ	33	33	33	32	31	24	29	
rOCNCβ	42	44	43	38	32	18		
hRCNCβ*	22	21	22	22	24			
tax-4	42	40	40	40				
dCNCα	43	46	47					
hCCNCα	62	61						
rOCNCα	59							
hRCNCα								

The coding regions of the channel subunits (for references on amino acid sequences, see Experimental Procedures) were aligned with the clustal V method of the MacAlign software from DNAstar. Each number represents the percentage of identical amino acid residues shared by two aligned sequences.
*For hRCNCβ, we have used the sequence of hRCNC2b (Chen et al., 1993), which is a truncated form of the β subunit, for the alignment.

it is quite likely that these two proteins will co-assemble with the subunits described in this work as well.

While three distinct α-subunits and two distinct β-subunits have been identified for the vertebrate cyclic-nucleotide-activated, nonselective cation channels to mediate visual transduction in rods and cones and olfactory transduction in olfactory cilia, so far only one each of α- and β-subunits have been identified in invertebrate species. In *Drosophila*, Southern blot analysis of genomic DNA has not led to any additional α-subunit genes (Baumann et al., 1994). In *C. elegans*, which has no photosensitive ocelli, the single α- and β-subunit genes identified appear to mediate olfactory, gustatory, and thermal sensations (Komatsu et al., 1996; Coburn and Bargmann, 1996). Thus, possibly, single ancient α- and β-subunit genes have multiplied into distinct but compatible copies during evolution, providing a greater diversity of channel properties to meet specific cellular functions.

Because all of the subunits can cross-assemble a variety of channel compositions, each with a unique set of properties, can be combinatorially generated from just a few α- and β-subunits. Besides heteromers involving one α-subunit species and one β-subunit species, there can, in principle, also be heteromers involving two or more α-subunit species, heteromers involving one α-subunit species and more than one β-subunit species, and so on. Whether this combinatorial diversity is indeed taken advantage of by the animal can only be revealed by examining the subunit compositions of native cyclic-nucleotide-activated channels found in cells and tissues other than sensory receptor cells (see Introduction). At a crude level, at least, existing information suggests that both the rod-channel β-subunit and the cone-channel α-subunit, but apparently not the rod-channel α-subunit, are expressed in the testis and heart (see Introduction); likewise, the olfactory-channel β-subunit, but apparently not the olfactory-channel α-subunit, is expressed in the vomeronasal organ (Berghard et al., 1996).

According to their amino acid sequences, the α- and β-subunits both have an overall structure resembling that of the *Shaker* superfamily of potassium channels, with six putative transmembrane domains (including an S4-like region), a putative β-hairpin forming part of the pore, and cytoplasmic N- and C-termini, with the C-terminus bearing the cyclic-nucleotide-binding domain (for reviews, see Kaupp, 1995; Finn et al., 1996; Zagotta and Siegelbaum, 1996). Functionally, the two families of ion channels also appear to be distant relatives (see, for example, Heginbotham et al., 1992). For the *Shaker* superfamily of potassium channels several subfamilies exist, with multi-gene members within each subfamily being able to co-assemble among themselves but unable to cross-assemble with those belonging to another subfamily, unless the molecular domain crucial for assembly is exchanged (Isacoff et al., 1990; Ruppersberg et al., 1990; Covarrubias et al., 1991; Sheng et al., 1993; Wang et al., 1993; Li et al., 1992; Shen and Pfaffinger, 1995; Xu et al., 1995; Jan and Jan, 1997). It will be interesting to see whether the same situation eventually applies to the cyclic-nucleotide-gated channels as well if new members are identified.

At the same time, as pointed out in the Introduction, there are other varieties of cyclic-nucleotide-gated cation channels beside those that are nonselective among cations and examined here. Thus, cyclic-nucleotide-activated channels that are selective for potassium have been described in native tissues (Delgado et al., 1991, 1995; Gomez and Nasi, 1995; Hatt and Ache, 1994; Labarca et al., 1996). Based on recent cDNA cloning, a channel protein with this characteristic appears to be, interestingly, more homologous to the *Shaker* superfamily of potassium channels than to the cyclic-nucleotide-activated, nonselective cation channels (Yao et al., 1995). Nonetheless, it would be interesting to see whether or not this protein can assemble with the sensory channel subunits described in this paper. Another variety, namely cyclic-nucleotide-inhibited cation channels, has been described in the apical membrane of renal inner medullary collecting duct cells as well as certain taste receptor cells (Light et al., 1989; Ahmad et al., 1992; Kolesnikov and Margolskee, 1995). So far, however, only cDNAs coding cyclic-nucleotide-activated channel subunits that are either identical to, or probably orthologs of, the sensory channel subunits have been obtained from these locations (Ahmad et al., 1992; Karlson et al., 1995; Misaka et al., 1997). Thus,

yet unidentified channel proteins may also exist that co-assemble with the sensory channel subunits to give rise to the opposite gating property with cyclic nucleotide.

The authors are grateful to J. C. Bradley and K. G. Zinn (Caltech) for kindly providing the cDNA encoding rOCNCβ, to I. Mori (Kyushu University, Japan) for the nematode tax-4 cDNA, and to T. E. Hughes (Yale) for the GFP cDNA. The *L-cis*-diltiazem is a gift from Tanabe-Seiyaku Co. (Osaka, Japan). We thank M. Chalfie (Columbia University), M. Li (Johns Hopkins University), and A. Wei (Washington University) for stimulating discussions, R. D. Barber and M. E. Grunwald in our laboratory and M. Li for comments on the manuscript, J. Lai, J. Li and M. Dehoff for technical help. M. E. Grunwald has also provided critical help for the final assembly of the figures.

This work was supported in part by a fellowship from Deutsche Forschungsgemeinschaft (to D.K.) and National Eye Institute Grant EY 06837 (to K.-W. Y.).

REFERENCES

Ahmad, I., C. Korbmacher, A. S. Segal, P. Cheung, E. L. Boulpaep, and C. J. Barnstable. 1992. Mouse cortical collecting duct cells show non-selective cation channel activity and express a gene related to the cGMP-gated rod photoreceptor channel. *Proc. Natl. Acad. Sci. USA.* 89:10262–10266.

Ahmad, I., T. Leinders-Zufall, J. D. Kocsis, G. M. Shepherd, F. Zufall, and C. J. Barnstable. 1994. Retinal ganglion cells express a cGMP-gated cation conductance activatable by nitric oxide donors. *Neuron.* 12: 155–165.

Balasubramanian, S., J. W. Lynch, and P. H. Barry. 1996. Calcium-dependent modulation of the agonist affinity of the mammalian olfactory cyclic nucleotide-gated channel by calmodulin and a novel endogenous factor. *J. Membr. Biol.* 152:13–23.

Baumann, A., S. Frings, M. Godde, R. Seifert, and U. B. Kaupp. 1994. Primary structure and functional expression of a *Drosophila* cyclic nucleotide-gated channel present in eyes and antennae. *EMBO J.* 13: 5040–5050.

Berghard, A., L. B. Buck, and E. R. Liman. 1996. Evidence for distinct signaling mechanisms in two mammalian olfactory sense organs. *Proc. Natl. Acad. Sci. USA.* 93:2365–2369.

Biel, M., W. Altenhofen, R. Hullin, J. Ludwig, M. Freichel, V. Flockerzi, N. Dascal, U. B. Kaupp, and F. Hofmann. 1993. Primary structure and functional expression of a cyclic nucleotide-gated channel from rabbit aorta. *FEBS Lett.* 329:134–138.

Biel, M., X. Zong, M. Distler, E. Bosse, N. Klugbauer, M. Murakami, V. Flockerzi, and F. Hofmann. 1994. Another member of the cyclic nucleotide-gated channel family expressed in testis, kidney, and heart. *Proc. Natl. Acad. Sci. USA.* 91:3505–3509.

Biel, M., X. Zong, A. Ludwig, A. Sautter, and F. Hofmann. 1996. Molecular cloning and expression of a modulatory subunit of the cyclic nucleotide-gated cation channel. *J. Biol. Chem.* 271:6349–6355.

Bönigk, W., F. Müller, R. Middendorff, I. Weyand, and U. B. Kaupp. 1996. Two alternatively spliced forms of the cGMP-gated channel α-subunit from cone photoreceptor are expressed in the chick pineal organ. *J. Neurosci.* 16:7458–7468.

Bradley, J., J. Li, N. Davidson, H. A. Lester, and K. Zinn. 1994. Heteromeric olfactory cyclic nucleotide-gated channels: a subunit that confers increased sensitivity to cAMP. *Proc. Natl. Acad. Sci. USA.* 91: 8890–8894.

Bradley, J., Y. Zhang, R. Bakin, H. A. Lester, G. V. Ronnett, and K. Zinn. 1997. Functional expression of the heteromeric "olfactory" cyclic nucleotide-gated channel in the hippocampus: a potential effector of synaptic plasticity in brain neurons. *J. Neurosci.* 17:1993–2005.

Chen, T.-Y., M. Illing, L. L. Molday, Y.-T. Hsu, K.-W. Yau, and R. S. Molday. 1994. Subunit 2 (or β) of retinal rod cGMP-gated cation channel is a component of the 240-kDa channel-associated protein and mediates Ca^{2+}-calmodulin modulation. *Proc. Natl. Acad. Sci. USA.* 91:11757–11761.

Chen, T.-Y., Y.-W. Peng, R. S. Dhallan, B. Ahamed, R. R. Reed, and K.-W. Yau. 1993. A new subunit of the cyclic nucleotide-gated cation channel in retinal rods. *Nature.* 362:764–767.

Chen, T.-Y., and K.-W. Yau. 1994. Direct modulation by Ca^{2+}-calmodulin of cyclic nucleotide-activated channel of rat olfactory receptor neurons. *Nature.* 368:545–548.

Coburn, C. M., and C. I. Bargmann. 1996. A putative cyclic nucleotide-gated channel is required for sensory development and functions in *C. elegans*. *Neuron.* 17:695–706.

Covarrubias, M., A. Wei, and L. Salkoff. 1991. *Shaker, Shal, Shab,* and *Shaw* express independent K^+ current systems. *Neuron.* 7:763–773.

Delgado, R., P. Hidalgo, F. Diaz, R. Latorre, and P. Labarca. 1991. A cyclic AMP-activated K^+ channel in *Drosophila* larval muscle is persistently activated in dunce. *Proc. Natl. Acad. Sci. USA.* 88:557–560.

Delgado, R., R. Latorre, and P. Labarca. 1995. Selectivity and gating properties of a cAMP-modulated, K^+-selective channel from *Drosophila* larval muscle. *FEBS Lett.* 370:113–117.

Dhallan, R. S., J. P. Macke, R. L. Eddy, T. B. Shows, R. R. Reed, K.-W. Yau, and J. Nathans. 1992. Human rod photoreceptor cGMP-gated channel: amino-acid sequence, gene structure and functional expression. *J. Neurosci.* 12:3248–3256.

Dhallan, R. S., K.-W. Yau, K. A. Schrader, and R. R. Reed. 1990. Primary structure and functional expression of a cyclic nucleotide-activated channel from olfactory neurons. *Nature.* 347:184–187.

Feng, L., I. Subbaraya, N. Yamamoto, W. Baehr, and N. Kraus-Friedmann. 1996. Expression of photoreceptor cyclic nucleotide-gated cation channel α subunit (CNGCα) in the liver and skeletal muscle. *FEBS Lett.* 395:77–81.

Fesenko, E. E., S. S. Kolesnikov, and A. L. Lyubarsky. 1985. Induction by cyclic GMP of cationic conductance in plasma membrane of retinal rod outer segment. *Nature.* 313:310–313.

Finn, J. T., M. E. Grunwald, and K.-W. Yau. 1996. Cyclic nucleotide-gated ion channels: an extended family with diverse functions. *Annu. Rev. Physiol.* 58:395–426.

Frings, S., J. W. Lynch, and B. Lindemann. 1992. Properties of cyclic nucleotide-gated channels mediating olfactory transduction: activation, selectivity and blockage. *J. Gen. Physiol.* 100:45–67.

Frings, S., R. Seifert, M. Godde, and U. B. Kaupp. 1995. Profoundly different calcium permeation and blockage determine the specific function of distinct cyclic nucleotide-gated channels. *Neuron.* 15:169–179.

Gomez, M. D., and E. Nasi. 1995. Activation of light-dependent potassium channels in ciliary invertebrate photoreceptors involves cGMP but not the IP_3/Ca cascade. *Neuron.* 15:607–618.

Gordon, S. E., J. Downing-Park, and A. L. Zimmerman. 1995. Modulation of the cGMP-gated ion channel in frog rods by calmodulin and an endogenous inhibitory factor. *J. Physiol.* (*Lond.*). 486:533–546.

Gordon, S. E., and W. N. Zagotta. 1995a. Subunit interactions in coordination of Ni^{2+} in cyclic nucleotide-gated channels. *Proc. Natl. Acad. Sci. USA.* 92:10222–10226.

Gordon, S. E., and W. N. Zagotta. 1995b. Localization of regions affecting an allosteric transition in cyclic nucleotide-activated channels. *Neuron.* 14:857–864.

Goulding, E. H., G. R. Tibbs, and S. A. Siegelbaum. 1994. Molecular mechanism of cyclic nucleotide-gated channel activation. *Nature.* 372: 369–374.

Grunwald, M. E., W.-P. Yu, H.-H. Yu, and K.-W. Yau. 1998. Identification of a domain on the β-subunit of the rod cGMP-gated cation channel that mediates inhibition by calcium-calmodulin. *J. Biol. Chem.* In press.

Hackos, D. H., and J. I. Korenbrot. 1997. cGMP-gated channels of cone photoreceptors are modulated by an endogenous calcium binding molecule partially mimicked by calmodulin. *Biophys. J.* 72:115*a.* (Abstr.).

Hatt, H., and B. W. Ache. 1994. Cyclic nucleotide- and inositol phosphate-gated ion channels in lobster olfactory receptor neurons. *Proc. Natl. Acad. Sci. USA.* 91:6264–6268.

Haynes, L. W., and S. C. Stotz. 1997. Modulation of rod, but not cone, cGMP-gated photoreceptor channels by calcium-calmodulin. *Visual Neurosci.* 14:233–239.

Haynes, L. W., and K.-W. Yau. 1985. Cyclic GMP-sensitive conductance in outer segment membrane of catfish cones. *Nature.* 317:61–64.

Heginbotham, L., T. Abramson, and R. MacKinnon. 1992. A functional connection between the pores of distantly related ion channels as revealed by mutant K^+ channels. *Science*. 258:1152–1155.

Hsu, Y.-T., and R. S. Molday. 1993. Modulation of the cGMP-gated channel of rod photoreceptor cells by calmodulin. *Nature*. 361:76–79.

Isacoff, E. Y., Y. N. Jan, and L. Y. Jan. 1990. Evidence for the formation of heteromultimeric potassium channels in *Xenopus* oocytes. *Nature*. 345:530–534.

Jan, L. Y., and Y. N. Jan. 1997. Cloned potassium channels from eukaryotes and prokaryotes. *Annu. Rev. Neurosci*. 20:91–123.

Karlson, K. H., F. Ciampolillo-Bates, D. E. McCoy, N. L. Kizer, and B. A. Stanton. 1995. Cloning of a cGMP-gated cation channel from mouse kidney inner medullary collecting duct. *Biochim. Biophys. Acta*. 1236: 197–200.

Kaupp, U. B. 1995. Family of cyclic nucleotide-gated ion channels. *Curr. Opin. Neurobiol*. 5:434–442.

Kaupp, U. B., T. Niidome, T. Tanabe, S. Terada, W. Bönigk, W. Stûhmer, N. J. Cook, K. Kangawa, H. Matsuo, T. Hirose, T. Miyata, and S. Numa. 1989. Primary structure and functional expression from complementary DNA of the rod photoreceptor cyclic GMP-gated channel. *Nature*. 342:762–766.

Kingston, P. A., F. Zufall, and C. J. Barnstable. 1996. Rat hippocampal neurons express genes for both rod retinal and olfactory cyclic nucleotide-gated channels: novel targets for cAMP/cGMP function. *Proc. Natl. Acad. Sci. USA*. 93:10440–10445.

Kolesnikov, S. S., and R. F. Margolskee. 1995. A cyclic nucleotide-suppressible conductance activated by transducin in taste cells. *Nature*. 376:85–88.

Komatsu, H., I. Mori, J. S. Rhee, N. Akaike, and Y. Ohshima. 1996. Mutations in a cyclic nucleotide-gated channel lead to abnormal thermosensation and chemosensation in *C. elegans*. *Neuron*. 17:707–718.

Körschen, H. G., M. Illing, R. Seifert, F. Sesti, A. Williams, S. Gotzes, C. Colville, F. Müller, A. Dosé, M. Godde, L. Molday, U. B. Kaupp, and R. S. Molday. 1995. A 240 kDA protein represents the complete β-subunit of cyclic nucleotide-gated channel from rod photoreceptors. *Neuron*. 15:627–636.

Labarca, P., C. Santi, O. Zapata, E. Morales, C. Beltrán, A. Liévano, and A. Darszon. 1996. A cAMP-regulated K^+-selective channel from the sea urchin sperm plasma membrane. *Dev. Biol*. 174:271–280.

Li, M., Y. N. Jan, and L. Y. Jan. 1992. Specification of subunit assembly by the hydrophilic amino-terminal domain of the *Shaker* potassium channel. *Science*. 257:1225–1230.

Light, D. B., E. M. Schwiebert, K. H. Karlson, and B. A. Stanton. 1989. Atrial natriuretic peptide inhibits a cation channel in renal inner medullary collecting duct cells. *Science*. 243:383–385.

Liman, E. R., and L. B. Buck. 1994. A second subunit of the olfactory cyclic nucleotide-gated channel confers high sensitivity to cAMP. *Neuron*. 13:611–621.

Liu, D. T., G. R. Tibbs, and S. A. Siegelbaum. 1996. Subunit stoichiometry of cyclic nucleotide-gated channels and effects of subunit order on channel function. *Neuron*. 16:983–990.

Liu, M., T.-Y. Chen, B. Ahamed, J. Li, and K.-W. Yau. 1994. Calcium-calmodulin modulation of the olfactory cyclic nucleotide-gated cation channel. *Science*. 266:1348–1354.

Marshall, J., R. Molloy, G. W. J. Moss, J. R. Howe, and T. E. Hughes. 1995. The jellyfish green fluorescent protein: a new tool for studying ion channel expression and function. *Neuron*. 14:211–215.

Misaka, T., Y. Kusakabe, Y. Emori, T. Gonoi, S. Arai, and K. Abe. 1997. Taste buds have a cyclic nucleotide-activated channel, CNGgust. *J. Biol. Chem.* 272:22623–22629.

Nakamura, T., and G. H. Gold. 1987. A cyclic nucleotide-gated conductance in olfactory receptor cilia. *Nature*. 325:442–444.

Perry, R. J., and P. A. McNaughton. 1991. Response properties of cones from the retina of the tiger salamander. *J. Physiol. (Lond.)*. 433: 561–587.

Picones, A., and J. I. Korenbrot. 1995. Permeability and interaction of Ca^{2+} with cGMP-gated ion channels differ in retinal rod and cone photoreceptors. *Biophys. J*. 69:120–127.

Ruiz, M. L., B. London, and B. Nadal-Ginard. 1996. Cloning and characterization of an olfactory cyclic nucleotide-gated channel expressed in mouse heart. *J. Mol. Cell. Cardiol* 28:1453–1461.

Ruppersberg, J. P., K. H. Schröter, B. Sakmann, M. Stocker, S. Sewing, and O. Pongs. 1990. Heteromultimeric channels formed by rat brain potassium-channel proteins. *Nature*. 345:535–537.

Shen, N. V., and P. J. Pfaffinger. 1995. Molecular recognition and assembly sequences involved in the subfamily-specific assembly of voltage-gated K^+ channel subunit proteins. *Neuron*. 14:625–633.

Sheng, M., Y. J. Liao, Y. N. Jan, and L. Y. Jan. 1993. Presynaptic A-current based on heteromultimeric K^+ channels detected in vivo. *Nature*. 365:72–75.

Tibbs, G. R., E. H. Goulding, and S. A. Siegelbaum. 1997. Allosteric activation and tuning of ligand efficacy in cyclic nucleotide-gated channels. *Nature*. 386:612–515.

Wang, H., D. D. Kunkel, T. M. Martin, P. A. Schwartzkroin, and B. L. Tempel. 1993. Heteromultimeric K^+ channels in terminal and juxtaparanodal regions of neurons. *Nature*. 365:75–79.

Weyand, I., M. Godde, S. Frings, J. Weiner, F. Müller, W. Altenhofen, H. Hatt, and U. B. Kaupp. 1994. Cloning and functional expression of a cyclic nucleotide-gated channel from mammalian sperm. *Nature*. 368: 859–863.

Xu, J., W. Yu, Y. N. Jan, L. Y. Jan, and M. Li. 1995. Assembly of voltage-gated potassium channels: conserved hydrophilic motifs determine subfamily-specific interactions between the α-subunits. *J. Biol. Chem*. 270:24761–24768.

Yao, X., A. S. Segal, P. Welling, X. Zhang, C. M. McNicholas, D. Engel, E. L. Boulpaep, and G. V. Desir. 1995. Primary structure and functional expression of a cGMP-gated potassium channel. *Proc. Natl. Acad. Sci. USA*. 92:11711–11715.

Yau, K.-W., and K. Nakatani. 1985. Light-suppressible, cyclic GMP-sensitive conductance in the plasma membrane of a truncated rod outer segment. *Nature*. 317:252–255.

Yu, W.-P., M. E. Grunwald, and K.-W. Yau. 1996. Molecular cloning, functional expression and chromosomal localization of a human homolog of the cyclic nucleotide-gated ion channel of retinal cone photoreceptors. *FEBS Lett*. 393:211–215.

Zagotta, W. N., and S. A. Siegelbaum. 1996. Structure and function of cyclic nucleotide-gated channels. *Annu. Rev. Neurosci*. 19:235–263.